Supporting Information

Callura et al. 10.1073/pnas.1203808109

SI Results and Discussion

GFP Expression from Riboregulator Variant RR42. We observed an ~70-fold change in fluorescence when inducing GFP with the RR42 riboregulator variant (Fig. 2*B*). We deemed this expression range satisfactory; however, the maximum level of expression from the RR42 variant was two- to threefold lower than the level observed from the RR12y and RR12 riboregulators. There are two possible sources for this difference, both of which concern translation rates: differences in ribosomal-binding site (RBS) strengths and differences in *cis*-repressed mRNA (crRNA)–*trans*-activating RNA(taRNA) binding dynamics.

As described in the main text, to create the riboregulator RR42, we replaced the RBS in the RR12 variant with an RBS identified via the RBS Calculator (1). Although the replacement RBS did not have a lower predicted strength, the possibility exists that the RBS in the RR42 variant is weaker in vivo than the RBS in the RR12 variant. Lower RBS strength will result in lower translation initiation rates and lower GFP production.

Mutations in the RBS required mutations in the *cis*-repressive sequence to maintain the high degree of complementarity between the *cis*-repressive sequence and RBS. Thus, in constructing the RR42 variant, we mutated a number of bases in the *cis*-repressive sequence in addition to the RBS mutations. However, these mutations in the *cis*-repressive sequence were not simply one-for-one changes to complement each RBS mutation. As described previously, we generated dispersed bulges in the crRNA structure by introducing mismatches between the *cis*-repressive sequence and RBS (2). These bulges promote an open crRNA complex that enables the *cis*-repressive sequence to interact with the *trans*-activating sequence. Without these bulges, the high crRNA stability discourages the formation of the crRNA–taRNA duplex. Therefore, when mutating bases in the *cis*-repressive sequence of the RR42 variant to complement the replacement RBS, we attempted to preserve the number and distribution of dispersed bulges in the parent variant RR12. Balancing the preservation of the prototypical crR12 structure with the maintenance of *cis*-repressive sequence–RBS complementarity resulted in an unexpectedly high number of mutations. All together, we made 10 mutations to the *cis*-repressive sequence of the RR12 riboregulator to create the RR42 variant. With this many mutations, changes in crRNA–taRNA binding dynamics may have been responsible for the decrease in GFP expression from the RR42 variant. Decreased rates of open crRNA complex formation or lower crRNA–taRNA duplex stability will affect translation initiation negatively and thus will affect GFP production.

Regardless of the cause, the lower maximum expression from the RR42 riboregulator did not affect switchboard performance. Unintended GFP expression from crR42 and orthogonal taRNA molecules was minimal and similar to that of the RR12y and RR12 control plasmids (Fig. 2 *B–D*). In our switchboard sensor, the RR42 variant was responsible for a nearly 200-fold jump in GFP levels (Fig. 3*B*), and in our metabolism switchboard Gnd activity increased by >50 times from the RR42 riboregulator on a medium-copy plasmid (Fig. 5*A*). For both switchboards, crosstalk had almost no effect on expression from the RR42 variant.

Effects of *Edd* Knockout on *Eda* Expression. The Entner–Doudoroff pathway (EDP) consists of two genes: *edd* and *eda* (3), encoding phosphogluconate dehydratase and 2-keto-3-deoxygluconate-6-phosphate aldolase, respectively. Although we chose to regulate *edd* with our metabolism switchboard, there would be no EDP activity without *eda* expression.

To knock out the *zwf* and *edd* genes, we removed the entire region between *zwf* and *edd* from the MG1655ProΔ*gnd*Δ*pgi* genome. However, this deletion created a potential complication, because *edd* and *eda* share a promoter, and the two other characterized *eda* promoters are located within the *edd* gene (4). Because the *zwf-edd* knockout left only one *eda* promoter intact, the resulting *eda* expression in the switchboard background had to be assessed.

The relative mRNA concentration of *eda* was calculated in addition to the *pgi*, *zwf*, *edd*, and *gnd* data presented in the main text. Unexpectedly, the relative *eda* mRNA concentration was slightly higher in the switchboard-regulated pathways than in the wild-type control (Fig. S1). Furthermore, there was no significant difference in relative mRNA abundance in each metabolic state of the switchboard. Thus, removing two of the three *eda* promoters in the MG1655ProΔ*gnd*Δ*pgi*Δ*zwf-edd* strain did not lead to a significant decrease in *eda* expression. This conclusion was strengthened by the large, switchboard-mediated increase in EDP activity (Fig. 5*A*). With impaired *eda* expression, EDP activity would have remained low or would have been nonexistent.

Nontargeted Metabolome Changes. Metabolomics analysis did pick up nontargeted effects of the metabolism switchboard. Nucleotide levels were enriched significantly in all switchboard samples compared with the wild-type control. Furthermore, nonnucleotide purines and pyrimidines were found at much smaller levels with the switchboard, and de novo nucleotide synthesis intermediates were affected greatly. It is possible that maintaining the switchboard plasmids and producing a large number of RNA species affect nucleotide biosynthesis. In addition, long-chain fatty acids and many major phospholipid membrane components had significantly lower levels in the switchboard background. These changes point toward decreased cell membrane biosynthesis and an altered growth pattern. On a related note, wild-type cells had a higher growth rate than switchboard-containing cells (Fig. 3*D*).

SI Materials and Methods

Strains and Reagents. For experimental purposes, two related *Escherichia coli* K-12–derivative strains were used: MG1655Pro (F-, λ-, Sp^R, *lacR*, *tetR*) (5) and MG1655ProΔ*gnd*Δ*pgi*Δ*zwf-edd*. For cloning purposes, MG1655Pro and New England Biolabs 10-β–competent *E. coli* (*araD139* Δ(*ara-leu*)7697 *fhuA lacX74 GalK* (ϕ80 Δ(*lacZ*)*M15*) *mcrA galU recA1 endA1 nupG rpsL* (Str^R) Δ(*mrr-hsdRMS-mcrBC*) were used. To make the MG1655ProΔ*gnd*Δ*pgi*Δ*zwf-edd* strain, P1 transduction was used to transfer the *gnd::kanR* cassette from the Keio *E. coli* single-gene knockout library to MG1655Pro (6). The *kanR* gene subsequently was excised using the PCP20 λ recombinase system (7). Again, P1 transduction was used to transfer the *pgi::kanR* cassette from the knockout library to MG1655Δ*gnd*, and PCP20 was used to remove *kanR*. Finally, an established, PCR-based protocol was used to remove the *zwf-edd* sequence from the MG1655ProΔ*gnd*Δ*pgi* genome (7). This protocol consisted of amplifying *kanR* from the PKD4 plasmid with knockout-specific primers (Table S1) and transforming the PCR product into the MG1655ProΔ*gnd*Δ*pgi* strain containing pKD46, a temperature-sensitive plasmid that produces λ recombinase (7). As before, *kanR* was excised from the resulting MG1655ProΔ*gnd*Δ*pgi*Δ*zwf-edd* strain with PCP20. In every step of the knockout process, cells were supplemented with fructose (Fisher) instead of glucose because of the effects of the knockouts on glucose metabolism. All knockouts were confirmed with PCR.

A combination of the following inducers and reagents were used: acyl-homoserine lactone (AHL; Sigma), mitomycin C (MMC; Sigma), 1,10-phenanthroline (Sigma), $MgCl_2$ (Fisher), anhydrotetracycline (aTc; Sigma), and isopropyl-β-D-thio-galactoside (IPTG; Fisher). Riboregulator characterization and switchboard sensor experiments were performed in selective lysogeny broth medium (Fisher), and metabolism switchboard experiments were performed in modified M9 minimal medium that was created according to the following recipe: 1× M9 minimal salts (BD Difco), 0.5% glucose (Fisher), 0.2% casamino acids (Fisher), 0.05 mM $MgSO_4$ (Fisher), and 0.1 mM $CaCl_2$ (Fisher).

Plasmid Construction. Basic molecular biology techniques were implemented as previously described (8). All riboregulator systems were based on the published design (2). All plasmids were built using restriction endonucleases and T4 DNA Ligase from New England Biolabs and were verified by restriction analysis. Plasmids were transformed using standard heat-shock protocols (8). Plasmid isolation was performed using QIAprep Spin Miniprep Kits (Qiagen). For switchboard sensor construction, cells were grown in selective medium: lysogeny broth medium (Fisher) supplemented with 30 μg/mL kanamycin (Fisher) and/or 100 μg/mL ampicillin (Sigma). For metabolism switchboard construction, cells were grown in Super Optimal Broth medium [20 g/L tryptone (BD Bacto), 5 g/L yeast extract (BD Bacto), 10 mM NaCl (Fisher), 2.5 mM KCl (Fisher), 10 mM $MgSO_4$, 10 mM $MgCl_2$] supplemented with 0.5% fructose, 30 μg/mL kanamycin, and/or 100 μg/mL ampicillin. Table S2 contains a complete list of plasmids used in this study.

To construct the riboregulator variants RR42 and RR12y, rationally designed sequences were synthesized from Integrated DNA Technologies using the Minigene service; these sequences consisted of only riboregulation-specific components: taRNA, taRNA promoter, crRNA, and crRNA promoter. By using the restriction enzymes XbaI and KpnI (New England Biolabs), the synthesized sequences were subcloned into a plasmid containing GFP, a high-copy origin (ColE1), and the kanamycin resistance marker, resulting in the RR42(12)G and RR12y(12)G riboregulator plasmids. To create the control plasmids used for testing orthogonality, a series of cloning steps was undertaken to replace the taRNA in each variant. For example, using the restriction enzymes XhoI and XbaI (New England Biolabs), taR42 from the RR42(12)G plasmid was replaced with taR12y, resulting in the RR42/12y(12)G plasmid. In the same manner, the RR42/12(12)G, RR12y/42(12)G, RR12y/12(12)G, RR12/42(12)G, and RR12/12y(12)G control plasmids were constructed.

The genetic switchboard for the present study consists of two plasmids, each containing two riboregulators, two different origins of replication, and two different resistance markers. For our switchboard sensor the two plasmids were RR12y(MM)luc-RR12(FF)Z and RR42(RII)G-RR10(LL)mC-A1, and for our metabolism switchboard the plasmids were RR12y(MM)mpgi-RR12(11)zwf and RR10(22)edd-RR42(RII)mgnd-A1. (The naming convention is explained in the legend of Table S2.) Constructing the individual riboregulators, all of which initially contained the high-copy origin ColE1 and *kanR*, was the first step in creating the switchboard plasmids. The second origin and resistance marker were introduced by substituting the medium copy origin p15A and *ampR* into the RR42(RII)G and RR10(22)edd plasmids. To combine two riboregulators onto one plasmid, the riboregulator-specific sequences (minus the origin and resistance marker) of the RR12(FF)Z, RR10(LL)mC, RR12(11)zwf, and RR42(RII)mgnd plasmids were amplified and inserted into the RR12y(MM)luc, RR42(RII)G-A1, RR12y(MM)mpgi, and RR10(22)edd-A1 plasmids, respectively. Finally, the relevant plasmids, each containing two riboregulators, were cotransformed via electroporation. The final genetic switchboard strains were selected on lysogeny broth + agar (Fisher) plates containing 15 μg/mL kanamycin and 50 μg/mL ampicillin.

Because our metabolism switchboard cannot be tested as directly as our switchboard sensor, plasmids with GFP and mCherry in place of the metabolic enzymes were constructed as well. Specifically, the testing riboregulators included RR12y(MM)G, RR12(11)mC, RR10(22)mC, RR42(RII)G, RR12y(MM)G-RR12(11)mC, and RR10(22)mC-RR42(RII)G-A1. These plasmids enabled quick troubleshooting of the riboregulation scheme controlling metabolic enzyme expression.

All together, we used the following parts: *luxR*, pLuxI, P_{LlexO}, P_{LfurO}, pMgrB, $P_{LtetO-1}$, $P_{LlacO-1}$, *gfpmut3b*, *mCherry*, *lacZ*, *luc*, *mpgi*, *zwf*, *edd*, and *mgnd*. *luxR* and pLuxI are involved in the quorum-sensing pathway of *Vibrio fischieri* (9). When activated by AHL, the regulator LuxR then activates expression from pLuxI. P_{LlexO} and P_{LfurO} are modified versions of the λ phage P_L promoter containing two LexA and Fur operator sites, respectively (10). pMgrB was amplified from the MG1655 genome and is controlled by the Mg^{2+}-sensitive PhoPQ two-component system (11). $P_{LtetO-1}$ and $P_{LlacO-1}$ also are modified versions of the native bacteriophage λ P_L promoter containing two TetR and LacR operator sites, respectively (5). *gfpmut3b* and *mCherry* are fluorescent proteins (12, 13), and *lacZ* and *luc* are colorimetric and luminescent reporters, respectively. *mCherry* was modified via PCR to remove a potential second ribosome-binding site within the coding sequence. The metabolic enzyme genes *pgi, zwf, edd,* and *gnd* were amplified from the MG1655Pro genome. To aid in transferring these genes into the riboregulator system, recognition sites for the restriction enzyme Kpn1 were removed from *pgi* and *gnd* via site-directed mutagenesis (kit from Finnzymes) to generate the *mpgi* and *mgnd* genes. The *pgi* and *gnd* amino acid sequences were kept intact, and the mutated bases were not near the reported active sites of the enzymes. The mutagenesis primers are presented in Table S3.

PCR amplification was performed using the PTC-200 PCR machine (Bio-Rad) with Phusion High-Fidelity DNA polymerase (New England Biolabs). Oligonucleotide primers were purchased from Integrated DNA Technologies. The DNA sequences for *luxR* and pLuxI were synthesized by Integrated DNA Technologies and based on the GenBank M19039 sequence (14). The P_{LlexO} and P_{LfurO} sequences were obtained from our DNA-damage and iron-regulation sensors (10). The $P_{LtetO-1}$ and *gfpmut3b* sequences were obtained from our original riboregulator system (2). The $P_{LlacO-1}$ sequence was obtained from the pZ plasmid system (5). mCherry was purchased from Clontech. The *lacZ* sequence was amplified from the MG1655Pro genome. The *luc* sequence was obtained from the pGEM-luc plasmid (Promega).

Riboregulator Variant Characterization. The synthetic riboregulator variants RR42 and RR12y were characterized by comparing their range of expression and the amount of unintended expression from orthogonal taRNA with the parent variant RR12. All variants riboregulated the expression of GFP and drove the transcription of the crRNA and taRNA with $P_{LtetO-1}$ and $P_{LlacO-1}$, respectively. MG1655Pro cells containing a synthetic riboregulator variant [RR42(12)G, RR12y(12)G, or RR12(12)G] or an orthogonality test plasmid [RR42/12y(12)G, RR42/12(12)G, RR12y/42(12)G, R12y/12(12)G, RR12/42(12)G, or RR12/12y(12)G] were grown overnight and then diluted 1:100 in 3 mL selective lysogeny broth medium (+30 μg/mL kanamycin). The appropriate cultures were induced at an OD_{600} ~0.3 (time 0), and samples were removed for flow cytometry analysis at 0, 1, 2, and 3 h postinduction. For each plasmid, the OFF state (no inducers) was compared with the ON state (full induction; + 100 ng/mL aTc + 1 mM IPTG). In addition, samples in which only the crRNA was expressed (+100 ng/mL aTc and no IPTG) were

analyzed for the RR42(12)G, RR12y(12)G, and RR12(12)G plasmids.

GFP fluorescence was measured using a Becton Dickinson FACSAria II flow cytometer. Specifically, data were collected with a 488-nm blue laser and 505- to 525-nm emission filter. The following photomultiplier (PMT) voltages were used: 353 forward scatter (FSC), 271 side scatter (SSC), and 457 (FITC). For each sample, 100,000 events were recorded, gated by an FSC and SSC threshold. Cells were washed and resuspended in 1× PBS before measurement. Fold-change values were calculated using the following formula: [ON state population mean]/[OFF state population mean].

Reporter Quantification. To measure the performance of the switchboard sensor, five samples were analyzed with different reagent concentrations representing the individual induction of the four reporters and the negative control (OFF state, zero reporters induced). For the Luciferase sample, MG1655Pro cells containing RR12y(MM)luc-RR12(FF)Z and RR42(RII)G-RR10(LL)mC-A1 were grown overnight and then diluted 1:100 in 15 mL selective lysogeny broth medium (containing 30 μg/mL kanamycin and 50 μg/mL ampicillin). Without excess $MgCl_2$, luciferase was induced from RR12y(MM)luc with no need for additional reagents. For the GFP, mCherry, LacZ, and negative control samples, MG1655Pro cells containing RR12y(MM)luc-RR12(FF)Z and RR42(RII)G-RR10(LL)mC-A1 were grown overnight and then were diluted 1:100 in a single volume of 65 mL selective lysogeny broth (containing 30 μg/mL kanamycin and 50 μg/mL ampicillin) plus 10 mM $MgCl_2$ to repress luciferase expression. At OD_{600} ~0.3–0.4, the 65-mL volume was split into four 15-mL samples. Inducers were added to the GFP, mCherry, and LacZ samples, but the negative control continued to only contain 10 mM $MgCl_2$. The concentrations of the inducers were 100 μM AHL [GFP induction from RR42(RII)G], 5 μg/mL MMC [mCherry induction from RR10(LL)mC], and 200 μM 1,10-phenanthroline [LacZ induction from RR12(FF)Z]. For all five samples, OD_{600} ~0.3–0.4 was time 0, and 625 μL were removed at 0, 1, 2, and 3 h for reporter quantification. The reporter assays were performed between time points and in the following order: β-galactosidase assay, luciferase assay, and flow cytometry.

β-Galactosidase Assay. LacZ activity was measured using the Yeast β-Galactosidase Assay Kit (Thermo Scientific) and a modified version of its Microcentrifuge Tube Protocol. This kit uses the color change resulting from the conversion of o-nitrophenyl galactoside to o-nitrophenol to measure activity. We made two major changes to the protocol. (*i*) The working solution contained assay buffer mixed with bacterial protein extraction reagent (Thermo Scientific), not yeast protein extraction reagent. (*ii*) Cells were washed and resuspended in 1× PBS (Fisher) to remove excess $MgCl_2$, which negatively affected protein extraction, from the medium before activity was measured. Absorbance values were measured with the SpectraMax M5 (Molecular Devices), and activity was calculated using the following formula: (1,000 * A420)/(t * V * OD_{600}), where *A420* was the measurement of the color change produced by β-galactosidase activity, *t* was the incubation time of cells with working solution (in minutes), *V* was the volume of cells in the assay (in milliliters), and OD_{600} was the optical density at 600 nm of cells used in the assay. Fold-change values were calculated using the following formula: [ON state activity]/[OFF state activity].

Luciferase Assay. Luciferase activity was measured using the Luciferase Assay System (Promega) and a modified version of its Protocol for Bacterial Cell Lysates and Protocol for Plate-Reading Luminometers. This kit uses the production of light from the conversion of beetle luciferin to oxyluciferin to measure luciferase activity. Cells (100 μL) were spun down and lysed by 15-min incubation in a water bath at room temperature with 300 μL lysis mix composed of 1× Cell Culture Lysis Reagent, 1.25 mg/mL lysozyme (Fisher), 2.5 mg/mL BSA (New England Biolabs), and water. After centrifugation for 2 min to remove debris, 20 μL cell lysate was added to 100 μL Luciferase Assay Reagent in a 96-well, white, round-bottomed plate (Corning). Luminescence of one sample at a time was measured for a reaction time of 1 min in the SpectraMax M5, and the reported value was normalized by the OD_{600} of cells used in the assay. Fold-change values were calculated using the following formula: [ON state normalized luminescence]/[OFF state normalized luminescence].

Flow Cytometry. GFP and mCherry fluorescence were measured using a Becton Dickinson FACSAria II flow cytometer. Specifically, GFP data were collected with a 488-nm blue laser and a 505- to 525-nm emission filter (FITC), and mCherry data were collected with a 561-nm yellow-green laser and a 600- to 620-nm emission filter (mCherry). The following PMT voltages were used: 353 (FSC), 271 (SSC), 457 (FITC), and 800 (mCherry). For each sample, 100,000 events were recorded, gated by an FSC threshold. Cells were washed and resuspended in 1× PBS before measurement. Fold-change values were calculated using the following formula: [ON state population mean]/[OFF state population mean].

Growth Conditions for Metabolic Analyses. In every metabolism switchboard analysis, modified M9 minimal medium was used. The recipe for the modified minimal medium was 1× M9 minimal salts, 0.5% glucose, 0.2% casamino acids, 0.05 mM $MgSO_4$, and 0.1 mM $CaCl_2$. The $MgSO_4$ concentration was 40 times lower than prescribed. pMgrB activity, and thus Pgi expression (Fig. 4*A*), was sensitive to Mg^{2+} concentration. Therefore, lowering the amount of $MgSO_4$ was necessary to maximize Pgi expression when targeting the Embden–Meyerhof pathway (EMP). Empirical observation found 0.05 mM to be the lowest $MgSO_4$ concentration that did not significantly impair cellular growth.

For each experiment, three metabolism switchboard samples, representing the EMP, EDP, and pentose phosphate pathway (PPP) metabolic states, were analyzed along with a wild-type control sample. MG1655Pro*Δgnd Δpgi Δzwf-edd* cells containing RR12y(MM)mpgi-RR12(11)zwf and RR10(22)edd-RR42(RII)mgnd-A1 were grown overnight in the EMP state and then were diluted 1:100 in 15 mL selective, modified M9 minimal medium (containing 30 μg/mL kanamycin and 100 μg/mL ampicillin). At inoculation, the following inducer concentrations were added to the relevant cultures: no inducers (EMP; Pgi ON); 10 mM $MgCl_2$, 30 ng/mL aTc, and 1 mM IPTG (EDP; Pgi OFF, Zwf ON, Edd ON); and 10 mM $MgCl_2$, 30 ng/mL aTc, and 100 μM AHL (PPP; Pgi OFF, Zwf ON, Gnd ON). In addition, MG1655Pro cells were grown overnight, and then were diluted 1:100 in 15 mL nonselective, modified M9 minimal medium. To analyze normal glucose metabolism in wild-type cells, no inducers were added to the control sample.

Quantitative PCR. ***cDNA preparation.*** To measure the performance of the metabolism switchboard at the RNA scale, the relative mRNA concentrations were measured for the target metabolic enzymes. Growth conditions for the collection of total RNA were as described above, and samples for quantitative PCR (qPCR) analysis were taken at OD_{600} ~0.8–0.9. Total RNA was obtained using the RNeasy Protect Bacteria Mini Kit (Qiagen), according to manufacturer's instructions. Briefly, RNA Protect (Qiagen) was added to culture samples, which then were pelleted by centrifugation at 3,000 × *g* for 15 min and stored overnight at −80 °C. Total RNA was extracted using the RNeasy kit, and samples were DNase treated using DNA-free (Ambion). Sample concentration was estimated using the ND-1000 spectropho-

tometer (NanoDrop). cDNA was prepared from 5 μg total RNA through random primed reverse transcription using SuperScript III (Invitrogen) and was purified with RNase H (Ambion) treatment.

Protocol. qPCR was performed using the Roche LightCycler 480. Using the LightCycler 480 SYBR Green I Master hot-start reaction mix (Roche) and following the manufacturer's instructions, we added the following reagents to a LightCycler 480 Multiwell Plate 96: (*i*) 50 ng cDNA template, (*ii*) SYBR Green 1, (*iii*) 5 μM forward and reverse qPCR primers, and (*iv*) PCR-grade water. The plate was sealed with sealing foil and spun down at 3,000 × *g* for 2 min before the qPCR reaction was started.

The qPCR program consisted of the following steps: preincubation, 45 amplification cycles, melting curve analysis, and a final cooling phase. Preincubation was run at 95 °C for 15 min. During amplification, the denaturation phase was run at 95 °C for 10 s, the annealing phase was run at 56 °C for 10 s, and the extension phase was run at 72 °C for 10 s. Melting curve analysis was run at 95 °C for 5 s, followed by 65 °C for 1 min, and finally at 95 °C until all DNA species had melted (continuously taking five acquisitions per second). The cooling phase was run at 40 °C for 30 s.

Analysis. The target genes were *pgi, zwf, edd, gnd*, and *eda*. When analyzing the qPCR data, the mean *lplT* and *rrsH* crossing point (C_P) values, determined with the second derivative maximum method (Roche Lightcycler 480 Instrument Operator's Manual, Software Version 1.5), were averaged to arrive at a single reference C_P value. The target/reference ratios (equal to the relative mRNA concentrations) were calculated using the following formula: $2^{\text{Target Cp}}/2^{\text{Reference Cp}}$ (Roche Lightcycler 480 Instrument Operator's Manual, Software Version 1.5). This formula assumes the PCR efficiencies equal 1 and the amounts of starting material in the reference and target reactions are equal. To determine the target gene mRNA percentages presented in Fig. 4*C*, the relative mRNA concentrations for *pgi, zwf, edd,* and *gnd* were added together for each metabolic state, and the percentage of each individual gene was calculated. For example, the the *pgi* target/reference ratio value for the EMP state was divided by the sum of the *pgi*, *zwf, edd,* and *gnd* target/reference ratio values for the EMP state. To determine the *eda* mRNA levels presented in Fig. S1, we scaled the raw target/reference ratios for *eda* by the minimum value of any gene in each trial.

Growth analysis. Exponential growth rate was measured using the growth conditions described above, with one change: Sample volume was 300 μL, not 15 mL, to allow samples to be grown in a 96-well, clear, flat-bottomed plate. OD_{600} was measured every 30 min, from 0–7 h, using the SPECTRAFluor Plus (Tecan).

Activity Assays. In all activity assays, the growth conditions described above were used, and all cell extracts were prepared in the following manner. Every step in the cell extract preparation protocol was performed on ice. At OD_{600} ~0.8–0.9, the 15-mL cultures were washed once and resuspended in 1 mL disruption buffer [0.9% (wt/vol) NaCl and 10 mM $MgSO_4$]. Cells were lysed with a microtip on the Branson Digital Sonifier. Each sample received 4- to 5-s pulses at 70% amplitude. After centrifugation for 10 min at 3,000 × *g* to remove cellular debris, lysate was transferred to a clean microcentrifuge tube and used immediately in the following protein concentration and activity assays. The protocols described below for measuring activity from cell lysate are based on Peng and Shimizu (15).

The Coomassie Plus Assay Kit (Pierce) was used to measure total protein concentration in the cellular lysates. This kit is an optimization of the Bradford Assay. Briefly, 10 μL lysate was mixed with 300 μL Coomassie Plus reagent in a 96-well, clear, flat-bottomed plate (Corning). The plate was shaken for 30 s, and the A595 of the lysate-reagent mixture was measured immediately with the SpectraMax M5. To calculate the total protein concentration, the A595 values were compared with a BSA (Pierce) standard curve that ranged from 0–2,000 μg/mL. The standard curve was fit by a fourth-order polynomial and was recalculated for each individual experiment.

To measure Gnd activity, the following reaction mixture was used: 100 mM Tris·HCl (pH 7.5) (Teknova), 6 mM $MgCl_2$, 1 mM $NADP^+$ (Sigma), 2 mM gluconate-6-phosphate (Sigma), and 1 mM DTT (Sigma). Fifty micrograms of total protein from each cell lysate sample was added to 1 mL Gnd reaction mixture. Immediately, the absorbance at 340 nm (A340) and 30 °C was measured in a 96-well, clear, flat-bottomed plate for 3 min using the SpectraMax M5, with measurements recorded every 15 s. Enzyme activity was calculated by measuring the slope of the resulting A340-vs.-time curve. The units of activity were converted to nanomolars per minute per milligram by comparing the A340 values to an NADPH (Fisher) standard curve. Zwf activity was measured in a similar fashion, with two important changes. The Zwf reaction mixture contained 100 mM Tris·HCl (pH 7.5), 6 mM $MgCl_2$, 1 mM $NADP^+$, 2 mM glucose-6-phosphate (Sigma), and 1 mM DTT. Also, less than 10 μg total protein was added to the reaction mixture for the EDP and PPP metabolic states. (In these samples, adding 50 μg total protein resulted in a nonlinear A340-vs.-time curve because of a dramatic, switchboard-mediated jump in Zwf activity.)

To measure EDP activity, the following reaction mixture was used: 200 mM Tris·HCl (pH = 7.2) (Teknova), 10 mM $MgSO_4$, and 5 mM gluconate-6-phosphate. Fifty micrograms of total protein from each cell lysate sample was added to 0.75 mL EDP reaction mixture, and the samples were incubated at 30 °C for 30 min and then at room temperature for 10 min with 500 μL 500 mM HCl containing 0.02% (wt/vol) 2,4-dinitrophenylhydrazine (Sigma). Then 1 mL 2M NaOH (Fisher) was added. Finally, A450 was measured in a 96-well, clear, flat-bottomed plate using the SpectraMax M5. Enzyme activity was calculated by dividing the A450 value by the 30-min reaction time. The units of activity were converted to nanomolars per minute per milligram by comparing the A450 values with a pyruvate (Fisher) standard curve.

Metabolic-Profiling. ***Sample preparation.*** All steps in preparing samples for metabolic-profiling were performed on ice. Growth conditions were as described above with two changes: Sample volume was 30 mL, not 15 mL, to satisfy the Metabolon cell-count requirement. Also, two additional samples were prepared: EMP > EDP and EMP > PPP. In these samples, carbon flux was switched from the EMP to the EDP and PPP at metabolic steady state (OD_{600} ~0.8–0.9),instead of after overnight incubation. At OD_{600} ~0.8–0.9, samples were washed and resuspended in 3 mL 1× PBS. Cells were pelleted by centrifugation at 3,000 × *g* and 4 °C for 3 min and were flash frozen in an ethanol-dry ice bath. Each sample was stored at −80 °C until six replicates per sample were prepared.

Protocol and analysis. Metabolon performed the metabolic profiling of the switchboard strains and wild-type control. Cells were stored at −80 °C until time of analysis. In addition to the supplied samples, technical replicates of the Client Matrix, a homogenous pool of all samples combined, were analyzed to assess data quality. The outline of the analysis was as follows: (*i*) samples were extracted with a standard solvent-extraction method; (*ii*) extracted samples were analyzed in parallel on liquid chromatography (LC)/MS and GC/MS platforms; (*iii*) instrument variability and total process variability were determined; (*iv*) peaks in the MS data were identified and compared with a metabolomic library; and (*v*) statistical analysis was performed on all the detected compounds of known identity.

The automated MicroLab STAR system (Hamilton Company) was used for sample extraction. The desired biochemicals were isolated from the protein fraction using a series of proprietary organic and aqueous solutions. To perform both LC and GC in

parallel, the biochemical extract was split into two fractions, and organic solvent was removed from each fragment using a TurboVap (Zymark). Both sets of samples were frozen and vacuum-dried to finalize preparation for LC and GC.

For GC/MS, prepared extracts were vacuum-dried again for at least 24 h and derivatized with bistrimethyl-silyl-triflouroacetamide under dried nitrogen. The 5% phenyl GC column had a temperature ramp from 40–300 °C over 16 min. A Thermo-Finnigan Trace DSQ fast-scanning single-quadrupole mass spectrometer was used to analyze the samples via electron impact ionization.

For LC/MS, two aliquots of the prepared extracts were again dried and reconstituted in acidic or basic LC solvents that contained a minimum of 11 injection standards at fixed concentrations. Through two independent injections using different columns, the aliquots were analyzed using acidic positive ion-optimized conditions or basic negative ion-optimized conditions. The acidic conditions were gradient eluted with water and methanol containing 0.1% formic acid, and the basic conditions were gradient eluted with water and methanol containing 6.5 mM ammonium bicarbonate. The LC and MS platforms used were a Waters ACQUITY UPLC and a Thermo-Finnigan LTQ mass spectrometer, respectively. MS included an electrospray ionization source and linear ion-trap mass analyzer, and the analysis alternated between MS and data-dependent MS/MS scans using dynamic exclusion. The back end of the Thermo-Finnigan LTQ mass spectrometer was Fourier transform ion cyclotron resonance. When ion counts exceeded 2 million, mass measurements were performed with high accuracy (errors <5 ppm). Ion counts lower than 2 million required MS/MS fragmentation.

To assess data quality, instrument and process variability were determined by calculating relative SDs (RSD). Instrument variability was derived from the RSD for the internal standards used in the mass spectrometer, and the process variability was derived from the median RSD for the biochemicals identified in 100% of the Client Matrix samples. The instrument variability was 6%, and the process variability was 13%. Both values were deemed acceptable. To address data quality further, quality control (QC)-specific samples were included in the analysis; QC compounds were even added to the test samples. QC samples were used to evaluate the process control for each study, and to assist data curation.

Peaks in the raw data files were found with proprietary peak-integration software. These data were compared with a library of purified standard and recurrent unknown entries to identify biochemicals. The library consisted of more than 1,000 commercially available purified standards. Matches between data and library entries were made by a combination of chromatographic properties and mass spectra. Curation procedures were performed to ensure the quality of the peak and metabolite identification. Briefly, these procedures included use of proprietary visualization and interpretation software to ensure accurate peak identification and, when evaluating library matches, removal of system artifacts, misassignments, and background noise.

For statistical analysis, the Welch's two sample *t* test was used to compare the statistical significance of differences in mean metabolite concentrations between the different metabolic states. A P value of 0.05 was chosen as the significance level. Also, the false-discovery rate (FDR) was estimated via the q value. The FDR was an attempt to measure the number of false positives (falsely discovered statistically significant differences) in a population of two sample *t* tests.

1. Salis HM, Mirsky EA, Voigt CA (2009) Automated design of synthetic ribosome binding sites to control protein expression. *Nat Biotechnol* 27:946–950.
2. Isaacs FJ, et al. (2004) Engineered riboregulators enable post-transcriptional control of gene expression. *Nat Biotechnol* 22:841–847.
3. Fraenkel D, Vinopal RT (1973) Carbohydrate metabolism in bacteria. *Annu Rev Microbiol* 27:69–100.
4. Murray EL, Conway T (2005) Multiple regulators control expression of the Entner-Doudoroff aldolase (Eda) of *Escherichia coli*. *J Bacteriol* 187:991–1000.
5. Lutz R, Bujard H (1997) Independent and tight regulation of transcriptional units in *Escherichia coli* via the LacR/O, the TetR/O and AraC/I1-I2 regulatory elements. *Nucleic Acids Res* 25:1203–1210.
6. Baba T, et al. (2006) Construction of Escherichia coli K-12 in-frame, single-gene knockout mutants: The Keio collection. *Mol Syst Biol*, 10.1038/msb4100050.
7. Datsenko KA, Wanner BL (2000) One-step inactivation of chromosomal genes in *Escherichia coli* K-12 using PCR products. *Proc Natl Acad Sci USA* 97:6640–6645.
8. Sambrook J, Fritsch EF, Maniatis T (1989) *Molecular Cloning: A Laboratory Manual* (Cold Spring Harbor Laboratory, Cold Spring Harbor, NY).
9. Sitnikov DM, Schineller JB, Baldwin TO (1995) Transcriptional regulation of bioluminescence genes from *Vibrio fischeri*. *Mol Microbiol* 17:801–812.
10. Dwyer DJ, Kohanski MA, Hayete B, Collins JJ (2007) Gyrase inhibitors induce an oxidative damage cellular death pathway in *Escherichia coli*. *Mol Syst Biol* 3:91.
11. Minagawa S, et al. (2003) Identification and molecular characterization of the Mg2+ stimulon of *Escherichia coli*. *J Bacteriol* 185:3696–3702.
12. Cormack BP, Valdivia RH, Falkow S (1996) FACS-optimized mutants of the green fluorescent protein (GFP). *Gene* 173:33–38.
13. Shaner NC, et al. (2004) Improved monomeric red, orange and yellow fluorescent proteins derived from Discosoma sp. red fluorescent protein. *Nat Biotechnol* 22: 1567–1572.
14. Devine JH, Countryman C, Baldwin TO (1988) Nucleotide sequence of the luxR and luxI genes and structure of the primary regulatory region of the lux regulon of *Vibrio fischeri* ATCC 7744. *Biochemistry* 27:837–842.
15. Peng L, Shimizu K (2003) Global metabolic regulation analysis for *Escherichia coli* K12 based on protein expression by 2-dimensional electrophoresis and enzyme activity measurement. *Appl Microbiol Biotechnol* 61:163–178.

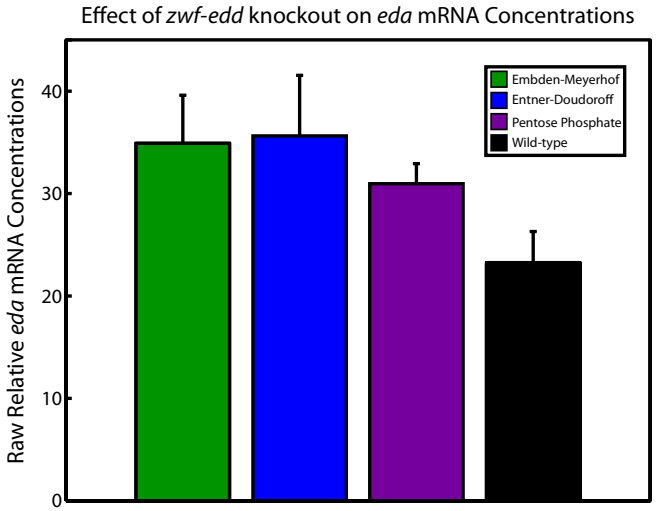

Fig. S1. *eda* expression in MG1655ProΔ*gnd*Δ*pgi*Δ*zwf-edd* background. Raw relative mRNA concentrations for the *eda* gene in different metabolic states. The graph depicts the triplicate mean ± SEM.

Table S1. Primers used in PCR knockout protocol when removing *zwf-edd* from the MG1655ProΔ*gnd*Δ*pgi* genome

Gene-specific sequence location	Primer sequence (5′ to 3′)
zwf	TTAGTTAACTTAAGGAGAATGACATGGCGGTAACGCGTGTAGGCTGGAGCTGCTTCG
edd	TAAGGAGGATATTCATATGGGGGCCAAAAGCGAACGGAATGCCAGAATTACATAA

Table S2. Plasmids used in the genetic switchboard study

Name	Cr variant	Ta variant	Cr promoter	Ta promoter	Target gene	Origin	Resistance marker
RR12(12)G	12	12	$P_{LtetO-1}$	$P_{LlacO-1}$	*gfp*	ColE1	*kanR*
RR12y(12)G	12y	12y	$P_{LtetO-1}$	$P_{LlacO-1}$	*gfp*	ColE1	*kanR*
RR42(12)G	42	42	$P_{LtetO-1}$	$P_{LlacO-1}$	*gfp*	ColE1	*kanR*
RR12/12y(12)G	12	12y	$P_{LtetO-1}$	$P_{LlacO-1}$	*gfp*	ColE1	*kanR*
RR12/42(12)G	12	42	$P_{LtetO-1}$	$P_{LlacO-1}$	*gfp*	ColE1	*kanR*
RR12y/12(12)G	12y	12	$P_{LtetO-1}$	$P_{LlacO-1}$	*gfp*	ColE1	*kanR*
RR12y/42(12)G	12y	42	$P_{LtetO-1}$	$P_{LlacO-1}$	*gfp*	ColE1	*kanR*
RR42/12(12)G	42	12	$P_{LtetO-1}$	$P_{LlacO-1}$	*gfp*	ColE1	*kanR*
RR42/12y(12)G	42	12y	$P_{LtetO-1}$	$P_{LlacO-1}$	*gfp*	ColE1	*kanR*
RR12y(MM)luc-RR12(FF)Z	12y; 12	12y; 12	pMgrB; P_{LfurO}	pMgrB; P_{LfurO}	*luc*; *lacZ*	ColE1	*kanR*
RR42(RII)G-RR10(11)mC-A1	42; 10	42; 10	*luxR*-pLuxI; $P_{LtetO-1}$	pLuxI; $P_{LtetO-1}$	*gfp*; *mCherry*	p15A	*ampR*
RR12y(MM)luc	12y	12y	pMgrB	pMgrB	*luc*	ColE1	*kanR*
RR12(FF)Z	12	12	P_{LfurO}	P_{LfurO}	*lacZ*	ColE1	*kanR*
RR42(RII)G	42	42	*luxR*-pLuxI	pLuxI	*gfp*	ColE1	*kanR*
RR10(11)mC	10	10	$P_{LtetO-1}$	$P_{LtetO-1}$	*mCherry*	ColE1	*kanR*
RR42(RII)G-A1	42	42	*luxR*-pLuxI	pLuxI	*gfp*	p15A	*ampR*
RR12y(MM)mpgi-RR12(11)zwf	12y; 12	12y; 12	pMgrB; $P_{LtetO-1}$	pMgrB; $P_{LtetO-1}$	*mpgi*; *zwf*	ColE1	*kanR*
RR10(22)edd-RR42(RII)mgnd-A1	10; 42	10; 42	$P_{LlacO-1}$; *luxR*-pLuxI	$P_{LlacO-1}$; pLuxI	*edd*; *mgnd*	p15A	*ampR*
RR12y(MM)mpgi	12y	12y	pMgrB	pMgrB	*mpgi*	ColE1	*kanR*
RR12(11)zwf	12	12	$P_{LtetO-1}$	$P_{LtetO-1}$	*zwf*	ColE1	*kanR*
RR10(22)edd	10	10	$P_{LlacO-1}$	$P_{LlacO-1}$	*edd*	ColE1	*kanR*
RR42(RII)mgnd	42	42	*luxR*-pLuxI	pLuxI	*mgnd*	ColE1	*kanR*
RR10(22)edd-A1	10	10	$P_{LlacO-1}$	$P_{LlacO-1}$	*edd*	p15A	*ampR*
RR12y(MM)G-RR12(11)mC	12y; 12	12y; 12	pMgrB; $P_{LtetO-1}$	pMgrB; $P_{LtetO-1}$	*gfp*; *mCherry*	ColE1	*kanR*
RR10(22)mC-RR42(RII)G	10; 42	10; 42	$P_{LlacO-1}$; *luxR*-pLuxI	$P_{LlacO-1}$; pLuxI	*mCherry*; *gfp*	ColE1	*kanR*
RR12y(MM)G	12y	12y	pMgrB	pMgrB	*gfp*	ColE1	*kanR*
RR12(11)mC	12	12	$P_{LtetO-1}$	$P_{LtetO-1}$	*mCherry*	ColE1	*kanR*
RR10(22)mC	10	10	$P_{LlacO-1}$	$P_{LlacO-1}$	*mCherry*	ColE1	*kanR*
RR42(RII)G	42	42	*luxR*-pLuxI	pLuxI	*gfp*	ColE1	*kanR*

Naming convention is as follows using RR42(12)G as an example: RR, riboregulator; 42, riboregulator variant; 1, $P_{LtetO-1}$ crRNA promoter; 2, $P_{LlacO-1}$ taRNA promoter; G, GFP target gene. Additional information that can be found in the naming convention includes: "/" indicating different crRNA and taRNA variants with the crRNA variant listed first; "-A" indicating p15A origin instead of ColE1 origin; "-1" indicating *ampR* instead of *kanR*; and "RR-RR" indicating two riboregulators on one plasmid with the host riboregulator listed first.

Table S3. Mutagenesis primers

Gene	Target codon	Primer sequences (5′ to 3′)
pgi	399	GGAACCAAAATGGTTCCGTGCGATTTCAT; GCGTTCTACCAGCTGATCCACCAG
gnd	124	TTTAACTTCATCGGCACCGGTGTTTCTGG; GTAATCGTGAGCTTTCAGCAGAGGGC
gnd	261	CGGCTAACAAAGGCACCGGTAAATGGA; GTAACTACCTGGTTGATGTGATCCTGGATGAAG

Primers used in site-directed mutagenesis protocol when removing Kpn1 recognition sites from the *pgi* and *gnd* genes. Two Kpn1 recognition sites were removed from the *gnd* gene.

Other Supporting Information Files

Dataset S1 (XLSX)